Liquid-Crystalline Solvents as Mechanistic Probes. 12. Solvent Anisotropy Effects on the Bending of Hydrocarbon Chains in α,ω-Bis(1-pyrenyl)alkanes[1]

Valerie C. Anderson and Richard G. Weiss*

Contribution from the Department of Chemistry, Georgetown University, Washington, DC 20057.
Received December 5, 1983

Abstract: A comparison has been made of the effects of the cholesteric and isotropic phases of a 59.5/15.6/24.9 (w/w/w) mixture of cholesteryl oleate/cholesteryl nonanoate/cholesteryl chloride (CM) and of the nematic and smectic phases of *trans,trans*-4′-*n*-butylbicyclohexyl-4-carbonitrile (BCCN) on the dynamics of intramolecular fluorescence quenching in several α,ω-bis(1-pyrenyl)alkanes (P*n*P). It is demonstrated that whereas the quenching activation parameters are independent of chain length (n = 3, 10, 13, 22) in the isotropic phase of CM, they vary greatly with chain length in cholesteric CM. Very little quenching of P3P or P22P fluorescence occurs in smectic BCCN. In nematic BCCN, the activation energy for quenching increases with increasing chain length. No intramolecular quenching of P7P was detectable in any of our solvent systems. From analyses of these results, we conclude that the nature of the influence of mesophase order on hydrocarbon chain bending depends in a subtle way upon the *length* of the chains. In isotropic media, bending efficiency is solvent dependent but solute chain length independent.

The dynamics of hydrocarbon chain bending has been examined theoretically and experimentally in isotropic media by several elegant methods.[2] The kinetics of the specific modes of bending which bring the ends of a chain within a critical distance can be examined indirectly from the rates of interaction between substituents appended to the head and tail. As the length of a hydrocarbon chain increases, so do the number of conformers available to it and the complexity of the system.

To understand better the factors governing chain bending in solution, several groups have measured the activation energy (E_a) associated with bringing a head and tail within an interaction distance as a function of chain length.[3] Surprisingly, the evidence indicates that E_a is independent of chain length when the chains are "long". For example, Shimada and Szwarc[4a] found that the activation energy for electron exchange between 1-naphthyl groups of α,ω-bis(1-naphthyl)alkanes in hexamethylphosphortriamide (HMPA) is constant for methylene chains containing from 5 to 20 carbons. Shimada, Shimozato, and Szwarc[4b] determined that activation energies for electron exchange between phthalimido groups of α,ω-bis(*N*-phthalimido)alkanes in HMPA decrease in a stepwise fashion as a function of chain length: for C_5–C_9 chains, E_a = 7.4 kcal/mol; for C_{10}–C_{16} chains, E_a = 6.7 kcal/mol. Rate differences within each set are due to progressive changes in the entropy of activation.[4b,5] In another example, Kanaya, Goshiki, Yamamoto, and Nishijima[5] observed that E_a for intramolecular fluorescence quenching of a series of bis((1-pyrenylmethoxy)-carbonyl)alkanes in 2-methyltetrahydrofuran is constant (5.1 ± 0.3 kcal/mol) for methylene chains of C_1 to C_{22}! In all of the examples, the activation energies are only slightly greater than the calculated potential energy barrier for hindered rotation about a single carbon–carbon bond.[6a] Thus, there is growing evidence that the rate-limiting step for attaining head-to-tail interactions in long, flexible chains involves rotation about one bond.[6b,c]

Each chain conformer, i, can be assigned a rate constant, r_i, for the head encountering the tail, so that the observed rate constant for head–tail interactions becomes R (eq 1) where x_i is the fraction of chains which exist on average in conformation i.[4a]

$$R = \sum_i x_i r_i \qquad (1)$$

When the head–tail interactions are specific r_i contains orientational factors, also. If all conformers interconvert rapidly or if one chain-common motion is rate limiting, R can be considered as a simple first-order rate constant. However, if internal or external (environmentally induced) constraints make difficult conversion of some families of conformers to others, the kinetics of interaction can become quite complex. Even without this complication, analyses of results can be very difficult since many conformers may be populated about equally in isotropic solvents: to determine the dynamics of bending of one conformer or a few conformers becomes experimentally impossible even if R simplifies to a first-order expression. In principle, analyses of kinetic data for head-to-tail motions would be simplified greatly if the distribution were narrowed to a few reasonably well-characterized chain conformers. This should be possible by exposing the chains to anisotropic interactions with suitably ordered solvent molecules. The anisotropic media serve two functions: to order solute chains with respect to neighboring solvent molecules and to influence the ease with which the chains undergo shape changes.

Previously, excimer/monomer fluorescence intensity ratios of 1,3-bis(1-pyrenyl)propane[7a,b] and 1,10-bis(1-pyrenyl)decane[7a,c] have been examined in micelles, multilayers, and vesicles. Lyotropic-phase transitions have been followed as a function of the same ratio but derived from (1,1′-dipyrenyl)methyl ether[8a] or from intermolecular interactions between pyrene[8b] or pyrenyl-substituted

(1) Part 11: Otruba, J. P., III; Weiss, R. G. *J. Org. Chem.* **1983**, *48*, 3448.
(2) For an excellent recent review, see: Winnik, M. A. *Chem. Rev.* **1981**, *81*, 491.
(3) The examples selected are for processes in which the intermolecular analogues are known to exhibit very low activation energies. When the activation barriers for head–tail interactions are much larger than those associated with chain bending, separation of the latter from the measured sum of the two becomes very difficult. For examples in which the activation energies for head–tail interactions are large, see citations in ref 2 and: Casadei, M. A.; Galli, C.; Mandolini, L. *J. Am. Chem. Soc.* **1984**, *106*, 1051.
(4) (a) Shimada, K.; Szwarc, M. *J. Am. Chem. Soc.* **1975**, *97*, 3313. (b) Shimada, K.; Shimozato, Y.; Szwarc, M. *Ibid.* **1975**, *97*, 5834. (c) Similar results have been obtained for intramolecular phosphorescence quenching of ω-alkenyl 4-benzoylbenzoates in carbon tetrachloride: Mar, A. Ph.D. Thesis, University of Toronto, 1982. *Diss. Abstr. Int. B*: **1983**, *43*, 3244B.
(5) Kanaya, T.; Goshiki, K.; Yamamoto, M.; Nishijima, Y. *J. Am. Chem. Soc.* **1982**, *104*, 3580. Yamamoto, M.; Goshiki, K.; Kanaya, T.; Nishijima, Y. *Chem. Phys. Lett.* **1978**, *56*, 333.
(6) (a) Piercey, J. E.; Rao, M. G. *J. Chem. Phys.* **1967**, *46*, 3951. (b) Liao, T.-P.; Morawetz, H. *Macromolecules* **1980**, *13*, 1228. (c) Perchak, D.; Weiner, J. H. *Ibid.* **1981**, *14*, 785.
(7) (a) Zachariasse, K. A.; Kuhnle, W.; Weller, A. *Chem. Phys. Lett.* **1980**, *73*, 6. (b) Kano, K.; Ishibashi, T.; Ogawa, T. *J. Phys. Chem.* **1983**, *87*, 3010. (c) Henderson, C. H.; Selinger, B. K.; Watkins, A. R. *J. Photochem.* **1981**, *16*, 215.
(8) (a) Georgescauld, D.; Desmasez, J. P.; Lapouyade, R.; Babeau, A.; Richard, H.; Winnik, M. *Photochem. Photobiol.* **1980**, *31*, 539. (b) Soutar, A. K.; Pownall, H. J.; Hu, A. S.; Smith, L. C. *Biochemistry* **1974**, *13*, 2828. (c) Sunamoto, J.; Kondo, H.; Nomura, T.; Okamoto, H. *J. Am. Chem. Soc.* **1980**, *102*, 1146. (d) Charlton, S. C.; Hong, K.-Y.; Smith, L. C. *Biochemistry* **1978**, *17*, 3304.

0002-7863/84/1506-6628$01.50/0

lecithins.[8c,d] The excimer/monomer ratio of pyrene in *N*-(*p*-methoxybenzylidene)-*p*-butylaniline is reported to be tenfold higher in the nematic phase than in the isotropic phase of the same solvent or in toluene; a brusque ratio change occurs at the phase-transition temperature.[8b] By contrast, we found that the excimer/monomer ratio of pyrene in a 59.5/15.6/24.9 (w/w/w) mixture of cholesteryl oleate/cholesteryl nonanoate/cholesteryl chloride (CM) increases from room temperature to above 70 °C.[9a] Furthermore, no large ratio change accompanies the cholesteric–isotropic phase transition.

In this work, we have dissolved several α,ω-bis(1-pyrenyl)alkanes (P*n*P, where n = 3, 7, 10, 13, and 22) in two relatively nonpolar solvents which exhibit liquid-crystalline phases. By comparing the rates and activation parameters of intramolecular pyrenyl singlet (^{1}P) quenching by a ground-state pyrenyl group (P, eq 2) as a function of solvent type and phase, we have been able to discern the influence of local solvent order on the dynamics of P*n*P. We find that the facility of chain motion is affected sig-

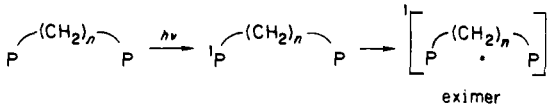

(2)

nificantly by solvent order in ways which are not prima facie obvious and which are in no way analogous to effects observed in isotropic media.

The cholesteric mixtures CM and BCCN (*trans,trans*-4′-*n*-butylbicyclohexyl-4-carbonitrile), which exhibits smectic and nematic mesophases, have been chosen as solvents for this work. The utility of CM in elucidating mechanistic details of intermolecular pyrene fluorescence quenching processes has been documented by us.[9] Additionally, we have used CM to examine the effect of solvent order on intramolecular pyrenyl fluorescence quenching in P3P[10] and in *N*,*N*-dimethyl-4-[3-(1-pyrenyl)-propyl]aniline.[11] BCCN-like solvents have been exploited by Samori et al. to investigate an intriguing thermal rearrangement.[12] Both BCCN and CM possess spectral and physical properties which make them excellent solvents for probing photophysical and photochemical processes in solutes which undergo large shape changes.

Experimental Section

Instrumental and general experimental procedures are as described previously[9-11] unless indicated otherwise. 1,3-Bis(1-pyrenyl)propane (P3P), mp 148–150 °C, 1-ethylpyrene (EP), mp 95–95.5 °C (lit.[13] mp 94–95 °C), and 1-dodecylpyrene (DP), mp 74.8–76.3 °C (lit.[14] mp 76 °C), were obtained from Molecular Probes and were used without further purification. 1,13-Bis(1-pyrenyl)tridecane (P13P), mp 125.5–127.5 °C, and 1,22-bis(1-pyrenyl)doeicosane (P22P), mp 132–133.5 °C, were donated by Dr. Klaas Zachariasse of the Max-Planck-Institut fur Biophysikalische Chemie, Gottingen. Analysis at 254 nm with a Waters HPLC Chromatograph using a Waters Rad-Pak B silica column and *n*-hexane as eluant showed EP to be greater than 99% pure. With an identical procedure, but 1/10 (v/v) chloroform/*n*-hexane as eluant, DP and P3P were estimated to be ca. 99% pure and P10P, P13P, and P22P were estimated to be greater than 95% pure. The impurities in the latter three compounds were not pyrene as discerned by chromatographic injections of an authentic sample.

Preparation of 1,7-Bis(1-pyrenyl)heptane (P7P). 1,7-Bis(1-pyrenyl)heptane was prepared by a modification of a published procedure.[15] Heptanedioic acid dichloride (from heptanedioic acid (Aldrich) and thionyl chloride), 10 mL, was added to 100 mL of freshly distilled methylene chloride containing 24.9 g (0.12 mol) of pyrene (K&K Laboratories; mp 150.5–151 °C after chromatography on silica using benzene as eluant and recrystallization from ethanol[16]). Approximately 9 g of anhydrous $AlCl_3$ was then added slowly to the chilled (−5 °C) solution. The reaction mixture was allowed to stand for ca. 30 min at 0 °C and then warmed to 10 °C. The slurry was poured into a concentrated HCl/ice mixture whereupon a yellow solid precipitated. The crude product was chromatographed on silica gel by using benzene as eluant and recrystallized to give 10.5 g (32%) of a pale yellow diketone product, mp 151–151.5 °C. IR (KBr) cm^{-1}: 3030, 2950, 1670 (m), 1665, 1620, 1610. After reduction of the diketone by a modification of the Huang–Minlon procedure,[17] the brown product was chromatographed on silica gel by using a 1/2 (v/v) benzene/petroleum ether eluant and then recrystallized 4 times from *n*-hexane to yield 0.05 g (5%) of a pale yellow crystalline product with mp 137–139.5 °C. IR (KBr) cm^{-1}: 3020, 2940 (s), 2860, 1600, 1590 (w), 1470 (m). HPLC analysis on a silica Rad-Pak B column (1/10 (v/v) chloroform/*n*-hexane) indicated a purity greater than 99%.

Transition Temperatures of CM and BCCN Mesophases. BCCN (Merck), $t_{s\rightarrow n}$ 54.5 °C, $t_{n\rightarrow i}$ 79.5 °C (lit.[18] $t_{s\rightarrow n}$ 54 °C; $t_{n\rightarrow i}$ 79 °C), displayed no detectable fluorescence. Cholesteryl oleate, cholesteryl nonanoate, and cholesteryl chloride were purified as previously described.[9b] A 59.5/15.6/24.9 (w/w/w/) mixture (CM) exhibited a cholesteric phase from below 25 °C to 58 °C.

Dynamic Measurements. The contribution (ca. 5%) of a short-lived component due to CM (τ < 7 ns) at the ^{1}P emission wavelength monitored (400 nm) necessitated subtraction of a CM blank from each sample decay.[10] Although some uncertainty in the ^{1}P lifetimes may have been introduced by this technique, the reproducibility of and systematic changes in the data indicate that the errors are not significant.[19]

Samples were prepared by adding a pyrenyl compound to CM or BCCN, each in its isotropic phase. Physical homogeneity of each sample was determined upon examination with a polarizing microscope. Aliquots were placed in flat Pyrex capillary tubes (0.4-mm width, i.d.) which were flame sealed after several freeze–pump–heat (to isotropic temperatures) cycles. Samples of 10^{-5} M EP and DP in cyclohexane (Fisher spectroanalyzed) were degassed and sealed at ca. 5×10^{-5} torr on a mercury-free vacuum line. Samples in CM were sealed at ≤0.1 torr, while those in BCCN were sealed at $\leq 5 \times 10^{-4}$ torr.

Lifetimes were measured on a single-photon counting apparatus described previously.[9b] Pyrenyl and excimer emissions were monitored at 400 nm and >500 nm, respectively. In order to improve signal to noise, sample cells were positioned at 45° to the excitation source in a thermostating holder (±0.5 °C, as determined with a calibrated thermistor). Counting times were empirical and were continued until at least 10 000 counts were registered in the peak channel and 1000 counts were registered in the last (tail) channel. For lifetime measurements in CM, the samples were allowed to equilibrate for 30–45 min at each cholesteric and isotropic temperature. However, in BCCN, it was found that sample equilibrium within the smectic phase required thermostating for *at least* 48 h prior to data collection if the material had been allowed to solidify previously. Shorter equilibration times resulted in irreproducible, complex decay curves due to solvent hysteresis. After initial equilibration in the smectic phase, incremental equilibrations at small temperature changes could be accomplished within 1 h. Fluorescence decay curves for all substituted pyrenes remained monoexponential over at least three half-lives in all equilibrated phases of CM and BCCN. All attempts to fit the decays to a double exponential led to unsatisfactory results: the amplitude associated with one of the decay constants invariably was negligible with respect to the other. In CM, decay constants were obtained from semilog plots of emission intensity vs. time over four regions

(9) (a) Anderson, V. C.; Craig, B. B.; Weiss, R. G. *J. Am. Chem. Soc.* **1982**, *104*, 2972. (b) Anderson, V. C.; Craig, B. B.; Weiss, R. G. *Ibid.* **1981**, *103*, 7169.

(10) Anderson, V. C.; Craig, B. B.; Weiss, R. G. *Mol. Cryst. Liq. Cryst.* **1983**, *97*, 351.

(11) Anderson, V. C.; Craig, B. B.; Weiss, R. G. *J. Phys. Chem.* **1982**, *86*, 4642.

(12) (a) Samori, B.; Fiocco, L. *J. Am. Chem. Soc.* **1982**, *104*, 2634. (b) Albertini, G.; De Maria, P.; Fanelli, E.; Poeti, G.; Rustichelli, F.; Samori, B.; Torquati, G. *Abstr. Int. Conf. Liq. Cryst. 9th, 1982* Bangalore, India, December 1982, Paper A-8. (c) De Maria, P.; Lodi, A.; Samori, B.; Rustichelli, F.; Torquati, G. *J. Am. Chem. Soc.* **1984**, *106*, 653.

(13) Josephy, E.; Radt, F., Eds. "Elsevier's Encyclopedia of Organic Chemistry"; Elsevier: New York, 1940; Series III, Vol. 14, p 379.

(14) Proske, T.; Fischer, C.-H.; Grätzel, M.; Henglein, A. *Ber. Bunsenges. Phys. Chem.* **1977**, *81*, 816.

(15) Zachariasse, K.; Kuhnle, W., *Z. Phys. Chem.* (*Neue* Folge) **1976**, *101*, 267.

(16) Birks, J. B.; Kazzazz, A. A.; King, T. *Proc. R. Soc. London, Ser. A* **1965**, *291*, 556.

(17) (a) Bell, R. A.; Ireland, R. E.; Partyka, R. A. *J. Org. Chem.* **1966**, *31*, 2530. (b) Abakerli, R. B. Ph.D. Thesis, Universidade de Sao Paulo, Brazil, 1976. (c) Abakerli, R. B.; Toscano, V. G.; Weiss, R. G. *J. Photochem.* **1981**, *15*, 229.

(18) "Licristal Liquid Crystals"; EM Chemicals: Hawthorne, New York, 1984.

(19) A constant (nonrandom) error was introduced into lifetime measurements of P13P and P22P by their impurities (which are probably 1-alkylpyrenes). The closeness between the lifetimes of our P13P and P22P in CM and those of 1-alkylpyrenes in the same solvent reduces these errors greatly and is responsible for our inability to separate the P13P and P22P decays into a sum of exponential functions. Regardless, the P13P and P22P lifetimes contain a slightly larger abolute error than the other P*n*P.

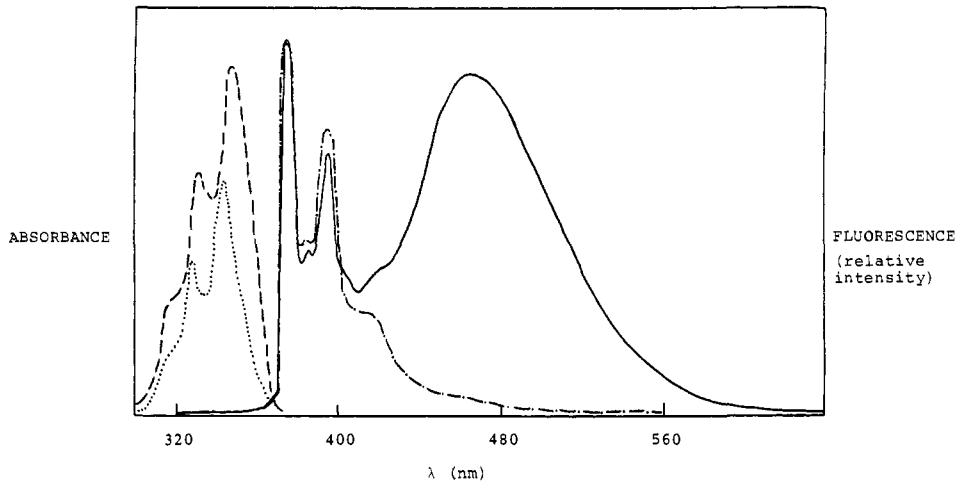

Figure 1. Uncorrected emission (λ_{excit} 310 nm; -----), excitation (λ_{emis} 400 nm; - - -) and absorption (...) spectra of 10^{-4} M P10P in degassed CM and emission spectrum (λ_{excit} 310 nm; —) of 10^{-5} M P10P in nitrogen-saturated *n*-hexane at 30 °C.

of each data set and varied by less than 2 ns (and were usually with 1 ns). No sample decomposition was detected, even after long counting times. Duplicate analyses on the same sample and on different samples of the same concentration indicated lifetimes were precise to within ±2 ns.

Decays in the smectic, nematic, and isotropic phases of BCCN were deconvoluted from the lamp pulse and analyzed by the method of moments.[20] Decay constants determined from linear semilog intensity vs. time plots and from the single exponential method of moments analysis were within 5%. Sample decomposition in BCCN and CM was negligible during counting and heating cycles, and lifetimes were easily reproduced at lower temperatures to within ±2 ns after isotropic-phase decay constants had been determined.

Liquid-Crystal-Induced Circular Dichroism (LCICD) Studies.[21] A 70/30 (w/w) mixture of cholesteryl nonanoate/cholesteryl chloride (CN/CCl) was homogenized and used as solvent. Solutions of pyrene, DP, P3P, P7P, and P10P in CN/CCl, each containing an equivalent concentration of pyrenyl chromophores (ca. 10^{-3} M), were prepared. Aliquots, sandwiched between 1-in.-diameter quartz plates separated by a 25-μm Teflon spacer, were placed in a thermostating cell[1,22] which had been installed in the sample compartment of a JASCO ORD/UV 5 (with a CD attachment) spectrophotometer. Circular dichroism spectra of the samples were recorded from ca. 220–600 nm in the cholesteric and isotropic phases of CN/CCl. A spectrum of undoped solvent was recorded for comparison purposes.

Results

Macroscopic Properties of BCCN and CM. The mesophases of BCCN and CM represent a wide variety of solvent order.[23] In a nematic phase, like that exhibited by BCCN from 54.5 °C to 79.5 °C, constituent molecules are oriented with their long axes approximately parallel but with no order about the individual centers of mass. A cholesteric mesophase (like CM from below room temperature to 58 °C[9b]) can be described as a macro-helical assembly of layers, each layer possessing nematic-like order, but being slightly twisted with respect to the ones above and below. A smectic phase, like that of BCCN from 28 °C to 54.5 °C, is more ordered than a nematic phase and, therefore, usually occurs at a lower temperature range.[24] Here, the mesophase is comprised of parallel, layered molecules which have their long molecular axes, on the average, at a nonzero angle to a layer plane. Microscopic observation of a distinctive mosaic texture[25] as well as a relatively high transition enthalpy from the crystalline to smectic phase ($\Delta H \simeq 4100$ cal/mol)[26] suggest a highly ordered B character for the smectic BCCN layers.

Transition temperatures were unaffected by the addition of 10^{-4} M P*n*P, EP, or DP to the neat solvents. However, at 0.1 M P3P, a substantial c → i temperature depression (10.5 °C) was observed for CM. These results and the small change in CM pitch (related to layer separations) which attends addition of 0.1 M P3P[10] suggest that *macroscopic* solvent order disruption by 10^{-4} M of a pyrenyl solute is slight.

A crude measure of the polarity of the microscopic environment of a pyrenyl group can be obtained from steady-state fluorescence measurements:[27] the ratio of the intensities of vibronic bands (III/I[9b]) is indicative of the site-averaged polarity of the environment in which the pyrenyl group is located. In CM, emission spectra of pyrene indicate it to be in a relatively nonpolar environments.[9b] In BCCN, the average local environment of the pyrenyl group is intermediate between that experienced in dodecane and *n*-butyl ether:[27b] III/I ≃ 1.4 for BCCN; III/I = 1.69[27b] (ε 2.00[28]) for dodecane; III/I = 1.19[27b] (ε 3.08[28]) for *n*-butyl ether.

Steady-State Spectra of P*n*P in CM and BCCN. Figure 1a contains the normalized emission, excitation, and absorption spectra of 10^{-4} M P10P in cholesteric CM at 30 °C. The similarity of the absorption and excitation spectra indicates that ground-state complexation is unimportant in cholesteric CM. Analogous spectra were obtained for all P*n*P[29] ($n \neq 7$; see below). Excitation spectra were recorded at many cholesteric temperatures and at several emission wavelengths (λ_{emis} 375, 385, 460, and 480 nm).

Our emission spectrum of 10^{-5} M P10P in *n*-hexane (Figure 1) compares favorably with that reported previously.[15] The broad, structureless emission shifted to the red of the ^{1}P emission is attributed to the intramolecular ^{1}P–P excimer. As was observed for P3P[10] and P3D,[11] our other P*n*P compounds (except $n = 7$, which has no discernible excimer emission) exhibit a ratio of intensity of intramolecular complex emission to ^{1}P emission which is substantially decreased relative to that observed in isotropic solvents. This is at least partially due to the relative high viscosity of the liquid-crystalline mesophases which hinder attainment of the excimer geometry within the ^{1}P excited-state lifetime. Typically, cholesteric phases are extremely syrupy, with viscosities that range from 10 to 10^3 P.[30] Smectic-phase viscosities are

(20) (a) Isenberg, I.; Dyson, R. D. *Biophys. J.* **1969**, *9*, 1337. (b) Isenberg, I.; Dyson, R. D.; Hanson, R. *Ibid.* **1973**, *13*, 1090.
(21) We thank Mr. Fabrizio Saraceni for performing these experiments.
(22) Otruba, J. P., III. Ph.D. Thesis, Georgetown University, Washington, DC, 1981.
(23) Kelker, H.; Hatz, R. "Handbook of Liquid Crystals"; Verlag Chemie: Deerfield Beach, FL, 1980.
(24) Petrie, S. E. B. In "Liquid Crystals: The Fourth State of Matter"; Saeva, F. D., Ed.; Marcel Dekker: New York, 1979.
(25) Demus, D.; Richter, L. "Textures of Liquid Crystals"; Verlag Chemie: New York, 1978.
(26) Licristal Catalog, E. Merck, Darmstadt, FDR, 1981.
(27) (a) Kalyanasundaraman, K.; Thomas, J. K. *J. Am. Chem. Soc.* **1977**, *99*, 2039. (b) Dong, D. C.; Winnik, M. A. *Photochem. Photobiol.* **1982**, *35*, 17. (c) Nakajima, A. *Bull. Chem. Soc. Jpn.* **1971**, *44*, 3272. *Spectrochim. Acta, Part A* **1974**, *30A*, 360.
(28) Riddick, J. A.; Bunger, W. B., Eds. "Techniques in Chemistry: Organic Solvents", 3rd ed.; Wiley-Interscience: New York, 1970; Vol. 2.
(29) Similar spectra of 10^{-4} M P3P in CM have been reported previously.[10]
(30) Porter, R. S.; Griffin, C.; Johnson, J. F. *Mol. Cryst. Liq. Cryst.* **1974**, *25*, 131.

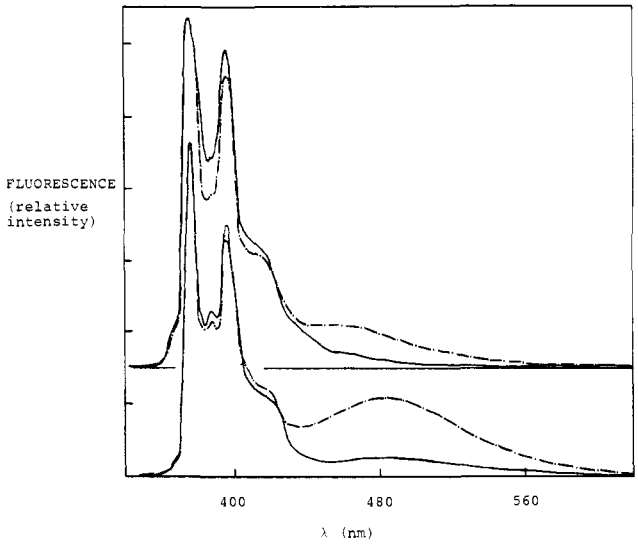

Figure 2. Uncorrected emission spectra (λ_{excit} 310 nm) of P3P (lower traces) and P10P (upper traces) in BCCN. (—) 48–49 °C (smectic); (----) 61 °C, (nematic).

usually between 10^2 and 10^3 cP,[31a] while those of nematics are $<10^2$ cP.[31b] Unfortunately, the absolute viscosities of cholesteric CM and of smectic and nematic BCCN[32] have not been determined. A correspondingly small ratio of excimer to monomer intensities has been observed for other bichromophorics in viscous isotropic,[33,34] polymeric,[33c,35] and micellar[36] solutions.

In addition to a decreased excimer emission intensity, comparison of the cholesteric spectra as a function of chain length reveals that the emission maxima in n = 10, 13, and 22 are blue-shifted relative to that observed for P3P ($\lambda_{max} \simeq 465$ nm for P10P, P13P, and P22P; $\lambda_{max} \simeq 480$ nm for P3P). Since these spectra are uncorrected and the intensity of complex emission is weak, no attempt has been made to quantify these observations. Nevertheless, the same trend with chain length appears to hold in BCCN. It has been suggested[15] that such blue shifts are due to the inability of the bis(pyrenyl)alkanes with intermediate chain lengths to achieve the optimal complex geometry.

Representative emission spectra of P10P and P3P in the smectic and nematic phases of BCCN are given in Figure 2. For both compounds, excimer emission is greatly reduced relative to the ^{1}P emission intensity, although intramolecular complex emission for P3P is apparent in both phases. As in CM, spectra were recorded at many smectic and nematic temperatures and several different emission wavelengths. Neither steady-state nor dynamic measurements revealed an excimer emission from 10^{-4} M P22P in smectic BCCN although, in the nematic phase, intramolecular excimer emission is observed. Apparently, the motions which are required to form a stable P22P excimer are sufficiently constrained by smectic BCCN to minimize formation of an emissive complex within τ', the lifetimes of ^{1}P.

As noted earlier, the emission spectrum of P7P in *n*-hexane and in CM is indistinguishable from that of EP or DP at concentrations where intermolecular events are negligible. Similarly, no P7P excimer emission was observed by Zachariasse[15] in methylcyclohexane. It has been suggested that this lack is due to unfavorable H–H interactions which occur during P7P chain folding.[2,15] However, comparison of CPK molecular models for several P*n*P indicates no obvious extraordinary interactions for P7P folding that we can discern.

Table I. LCICD Spectral Data for Pyrenyl Compounds in CN/CCl

solute	concn ×10⁶ (mol/g of CN/CCl)	temp,[a] °C	ΔA × 10³[b] 344 nm	ΔA × 10³[b] 242 nm
pyrene[c]	1.2	49	−6.3	−11.1
		61	−4.9	−9.0
		70	−3.3	−7.5
		80	0	0
DP	1.3	51	−5.0	−9.1
		61	−4.2	−7.5
P3P	0.59	51	−2.2	−3.6
		61	−1.7	−2.7
		70.5	−1.1	−1.6
		80	0	0
P7P	0.60	52	−2.6	−3.8
		62.5	−1.9	−2.8
		72	−1.4	−2.3
		80	0	0
P10P	0.59	49.5	−3.1	−5.5
		60	−2.4	−4.7
		70	−1.8	−3.1
		80	0	0

[a] ±1 °C. [b] The magnitudes of ΔA, the R and L light absorption difference, taken at 242 nm, especially, may have relatively large errors due to base-line uncertainties. A reasonable estimate of errors at 344 nm is ±5 × 10^{-4} absorbance unit; sample thickness is 25 μm. [c] Measurements at 238 and 335 nm.

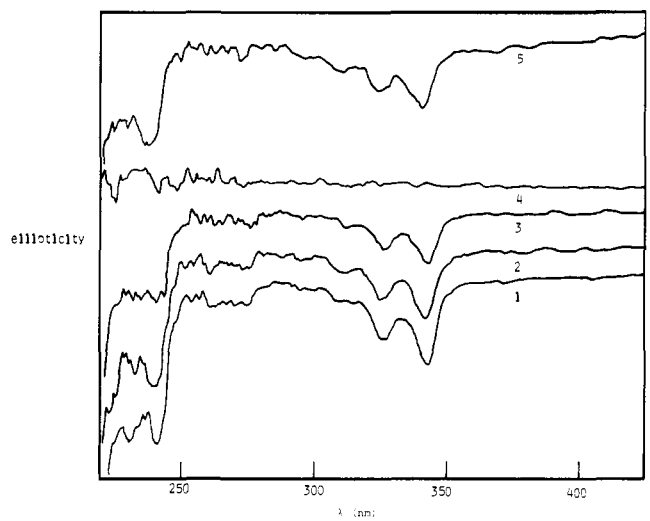

Figure 3. LCICD spectra of ca. 5 × 10^{-4} M P10P in CN/CCl taken in the sequence shown. (1) 50 °C (cholesteric); (2) 60 °C (cholesteric); (3) 70 °C (cholesteric); (4) 80 °C (isotropic); (5) 60 °C (cholesteric).

Liquid-Crystal-Induced Circular Dichroism (LCICD) Spectra in CN/CCl.[37] Our LCICD spectra of pyrene in CN/CCl correspond well with those published by Saeva, Sharpe, and Olin.[38] They noted that the 0–0 bands of the ^1L_b (too weak to be observed in our spectra) and the ^1B_b (277 nm) transitions show positive circular dichroism in CN/CCl (right-handed helix). The complete ^1L_a transition (0–0 band at 339 nm) shows a progression of vibronic bands which have negative circular dichroism. The polarization of the ^1L_a transition is known to lie along the long molecular axis of pyrene.[39] The polarization of the ^1B_b 0–0 band

(31) (a) Porter, R. S.; Barrall, E. M., II; Johnson, J. F. *J. Chem. Phys.* **1966**, *45*, 1452. (b) White, A. E.; Cladis, P. E.; Torza, S. *Mol. Cryst. Liq. Cryst.* **1977**, *43*, 13.
(32) Allen, F. V., EM Chemicals, private communication.
(33) (a) Avouris, P.; Kordas, J.; El-Bayoumi, M. A. *Chem. Phys. Lett.* **1974**, *26*, 373. (b) Ito, S.; Yamamoto, M.; Nishijima, Y. *Bull. Chem. Soc. Jpn.* **1981**, *54*, 35. (c) Wang, Y.-C.; Morawetz, H. *J. Am. Chem. Soc.* **1976**, *98*, 3611. (d) Ibemesi, J. A.; El-Bayoumi, M. A. *Mol. Photochem.* **1979**, *9*, 243.
(34) Yang, N. C.; Neoh, S. B.; Naito, T.; Ng, L.-K.; Chernoff, D. A.; McDonald, D. B. *J. Am. Chem. Soc.* **1980**, *102*, 2806.
(35) (a) Farid, S.; Martic, P. A.; Daly, R. C.; Thompson, D. R.; Specht, D. P.; Hartman, S. E.; Williams, J. R. *Pure Appl. Chem.* **1979**, *51*, 241. (b) Güsten, H.; Meisner, R.; Schoof, S. *J. Photochem.* **1980**, *14*, 77. (c) Tazuke, S.; Iwaya, Y.; Hayashi, R. *Photochem. Photobiol.* **1982**, *35*, 621.
(36) (a) Zachariasse, K. A. *Chem. Phys. Lett.* **1978**, *57*, 429. (b) Atik, S. S.; Thomas, J. K. *J. Am. Chem. Soc.* **1981**, *103*, 3550.
(37) Saeva, F. D. *Pure Appl. Chem.* **1974**, *38*, 25 and references cited therein.
(38) Saeva, F. D.; Sharpe, P. E.; Olin, G. R. *J. Am Chem. Soc.* **1973**, *95*, 7656.

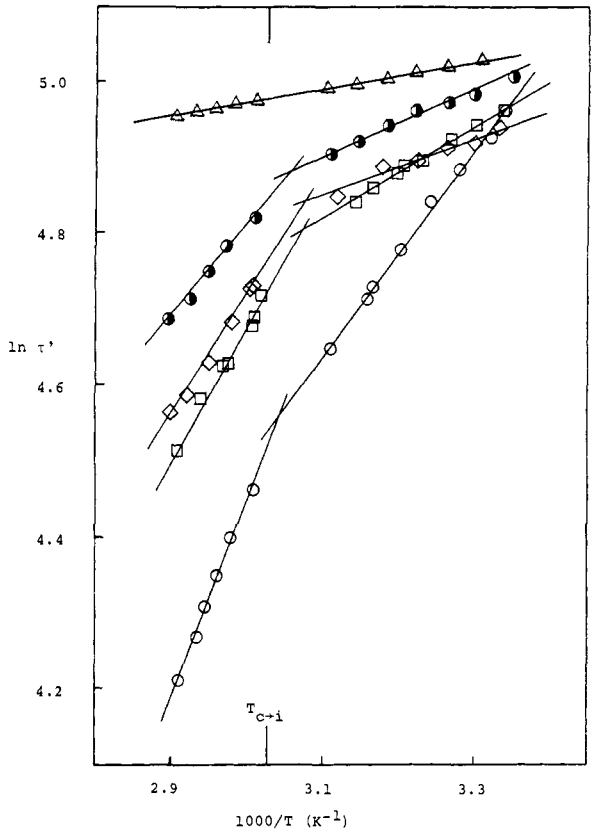

Figure 4. Arrhenius-type plots of singlet lifetimes in ns of 10^{-4} M P*n*P in CM. (○) P3P, (△) P7P, (◇) P10P, (□) P13P, (◑) P22P.

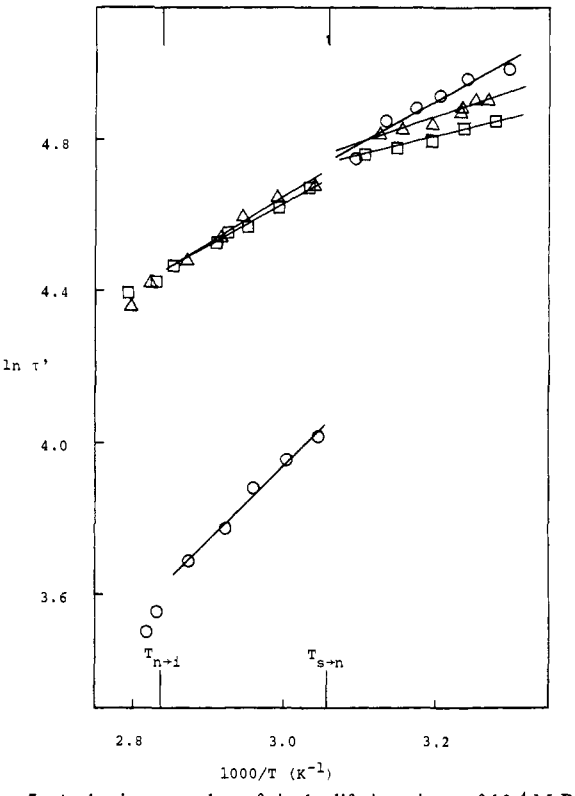

Figure 5. Arrhenius-type plots of singlet lifetimes in ns of 10^{-4} M P*n*P in BCCN. (○) P3P, (□) P10P, (△) P22P.

is polarized in the plane and perpendicular to the long molecular axis;[39] higher vibrations show negative circular dichroism and may belong to a mixed transition.[40] Sackmann et al.[41a] find from the Saupe order parameters that pyrene is oriented with its long molecular axis parallel to the long axes of the solvent molecules in a 1/1.85 (w/w) nematic point mixture of cholesteryl laurate/cholesteryl chloride. We are confident that pyrene in CN/CCl is oriented along the same direction. However, quantification of such assertions is limited by the degree of solvent perturbation on the symmetry of the transitions.[41b]

The P*n*P LCICD spectra in CN/CCl are very similar in appearance and exhibit ellipticities θ which are within experimental error of each other. Base lines for the spectra vary from sample to sample due to selective refraction of light. Therefore, the $\theta = 0°$ line was set in each run at the flat portion of the spectrum (600–400 nm). DP and pyrene in CN/CCl are spectrally shifted but exhibit corresponding LCICD bands which are similar in intensity (the $[\theta]$ for pyrene are ca. 30% higher than those of DP). After the DP, P3P, P7P, and P10P samples are normalized to reflect pyrenyl chromophore concentration instead of molecular concentration, the LCICD of DP is slightly more than twice as intense as that of P3P and P7P and slightly less than twice as intense as P10P. For all samples, the LCICD spectra disappear when CN/CCl becomes isotropic[38] (Table I). Representative LCICD spectra of P10P are presented in Figure 3.

The decreased spectral intensities of the P*n*P samples in comparison to the DP sample require that the order parameters of at least one pyrenyl group of each P*n*P be different from that of DP. Only if a P*n*P pyrenyl group contribution to the total $[\theta]$ was that of a DP pyrenyl group would $[\theta]$ for the bichromophorics be twice that of DP. Our measurements do not allow us to determine whether the order parameters of each of the pyrenyl groups of a P*n*P are the same or different. In effect, the LCICD measurement requires that the long axes of the pyrenyl groups in P3P, P7P, and P10P be, on average, less parallel to the long molecular axis of the cholesteric solvent molecules than is DP or pyrene.

Dynamic Measurements. Decay constants were measured in the cholesteric and isotropic phases of CM and in the smectic, nematic, and isotropic phases of BCCN at 10^{-4} M, where intermolecular events are unimportant.[10] The inverse of a ^{1}P decay constant is τ', its singlet lifetime (vide infra). Plots of the ln τ' vs. $1/T$ in CM and BCCN are given in Figures 4 and 5, respectively. In CM, all the P*n*P ($n \pm 7$) plots can be fit reasonably to two straight lines which intersect within 5 °C of, but are consistently lower than, the optically detected phase transition. We believe that the solutes create disorder in their surroundings which, in turn, depresses the *local* phase transition temperature. The P7P data exhibit linear, phase-independent behavior in CM (see Figure 4). In BCCN, the P*n*P data again can be approximated by phase-dependent straight lines which, for P10P and P22P, intersect near the optically detected smectic–nematic transition temperature. In the case of P3P, a large change in τ' is observed above $T_{s\to n}$, although the slopes of the two phases do not differ appreciably.

Kinetic Model for P*n*P Photophysics. A simple treatment for the photophysical processes of bichromophoric alkanes in nonpolar solvents is given in Scheme I.[2,42] The monolumophoric rate constants, k_1' and k_2', for each P*n*P are taken equal as a sum to the inverse of τ_M, the lifetimes of singlets of alkylpyrenes of approximately the same hydrocarbon chain length. Possible pseudo-first-order quenching by the fluorescing impurity in CM is incorporated in eq 5. Concentration-dependent lifetime studies (10^{-5}–5×10^{-4} M) of DP and EP[11] in the smectic and nematic phases of BCCN and the cholesteric and isotropic phases of CM indicate that bimolecular quenching is negligible at $\leq 10^{-4}$ M.

(39) (a) Hochstrasser, L. M. *J. Chem. Phys.* **1960**, *33*, 459. (b) Zimmermann, V. H.; Joop, N. *Z. Elektrochem.* **1960**, 138.
(40) (a) Horowitz, J.; Strickland, E. H.; Billups, C. *J. Am. Chem. Soc.* **1969**, *91*, 184. (b) Weigang, O. E., Jr. *J. Chem. Phys.* **1965**, *43*, 3609.
(41) (a) Sackmann, E.; Krebs, P.; Rega, H. U.; Voss, J.; Mohwald, H. *Mol. Cryst. Liq. Cryst.* **1973**, *24*, 283. (b) Langkilde, F. W.; Thulstrup, E. W.; Michl, J. *J. Chem. Phys.* **1983**, *78*, 3372.
(42) (a) DeSchryver, F. C.; Boens, N.; Put, J. *Adv. Photochem.* **1977**, *10*, 359. (b) Chandross, E. A.; Dempster, C. J. *J. Am. Chem. Soc.* **1970**, *92*, 3586. (c) Klöppfer, W. In "Organic Molecular Photophysics"; Birks, J. B., Ed.; Wiley: New York, 1975.

Scheme I. Simple Mechanism for Quenching of α,ω-Bis(1-pyrenyl)alkanes in Nonpolar Solvents

$$PnP \xrightarrow{h\nu} {}^1PnP \quad (3)$$

$${}^1PnP \xrightarrow{k_1'} PnP + h\nu' \quad (4)$$

$${}^1PnP \xrightarrow{k_2'} PnP + \Delta \text{ or } {}^3PnP \quad (5)$$

$${}^1PnP \underset{k_4'}{\overset{k_3'}{\rightleftharpoons}} {}^1(PnP) \quad (6)$$

$${}^1(PnP) \xrightarrow{k_5'} PnP + h\nu'' \text{ or } \Delta \quad (7)$$

As shown in Table II, the lifetimes of alkylpyrenes (τ_M) within a solvent are relatively insensitive to chain length.[43] In BCCN, τ_M was virtually constant throughout the entire temperature range of these measurements. In CM, a slight temperature dependence was observed. As a result, phase-dependent plots of τ_M vs. T were constructed and values of $k_1' + k_2'$ were extracted at each temperature for which τ' was determined.

Several pieces of experimental evidence lead us to conclude that each P*n*P in CM or BCCN represents one family of ground-state conformers separated by very low energy barriers for interconversion: (1) the lack of *measurable* deviation from monomer emission exponentiality; (2) the absence of a detectable dual component rise in the excimer wave forms; (3) the indistinguishability of the steady-state emission spectra for a P*n*P excited at several wavelengths; (4) the indistinguishability of the excitation spectra of a P*n*P spectrum monitored at several emission wavelengths; (5) and a correspondence between τ' and τ_D, the inverse of the decay constants obtained from the excimer waveforms. In other linked systems, nonmonoexponentiality of monomer and excimer wave-form decays, a nonunique manifestation of more than one energy-separated family of conformers, is reasonably well documented.[44] Recently, two detailed (and differing) discussions of dual conformer families for P3P in isotropic solvents have been published.[45]

In all P*n*P, except one, for which comparisons were possible, τ' from ^{1}P decays were much longer than the rise times calculated from the excimer wave forms: although the rise time and τ' of P3P in nematic BCCN were comparable, the monomer and excimer decays were exponential. Then since the rise times reflect the excimer decay times, τ_E',[10] the sum of the rate constants for the loss of ^{1}P is smaller than the sum for loss of excimer. The mechanistic ramifications of these inequalities and the observed exponentiality can be demonstrated with the time-dependent solutions to the coupled differential rate equations for ^{1}P and ^{1}(PnP) (eq 8–11) derived from Scheme I.[46] In these equations, $X = k_1'$ $+ k_2' + k_3'$, $Y = k_4' + k_5'$, K and K' are constants, and λ_1 and λ_2 are decay constants.

$$[^1P]_t = K(e^{-\lambda_1 t} + Ae^{-\lambda_2 t}) \quad (8)$$

$$[^1(PnP)]_t = K'(e^{-\lambda_1 t} - e^{-\lambda_2 t}) \quad (9)$$

$$\lambda_{1,2} = \tfrac{1}{2}[X + Y \mp [(X - Y)^2 + 4k_3'k_4']^{1/2}] \quad (10)$$

$$A = (X - \lambda_1)/(\lambda_2 - X) \quad (11)$$

Monoexponentiality for decay of ^{1}P in eq 8 requires that either $A \gg 1$ or $A \to 0$. Several experimental observations lead to one of these limits. Most important among these are that (1) the decay constants for ^{1}P and excimer clearly indicate that $Y > X$, and (2) the high-solvent viscosities and lack of observable changes in τ_E' within a phase of BCCN or CM, even though k_4' is known to be temperature dependent,[7,10,47] provide evidence that $k_5' \gg k_4'$ (i.e., $Y \simeq k_5'$).[48] A similar temperature independence for τ_E' of P3P has been noted in phosphatidylcholine bilayers from 10–50 °C.[7a] Therefore, $[X - Y]^2 \gg 4k_3'k_4'$ and λ_1 becomes $^1/_2[X + Y - |X - Y|]$ or $k_1' + k_2' + k_3'$. Similarly, A approaches $[X - Y - |X - Y|]/[Y - X + |X - Y|]$ or zero. With these simplifications, eq 8 can be expressed as eq 12, a monoexponential functional in which $\tau' = 1/X$. Equation 9 becomes eq 13, a combination of an

$$[^1P]_t \simeq Ke^{-Xt} = Ke^{-t/\tau'} \quad (12)$$

exponential decay and an exponential rise in which $\tau_E' = 1/Y$.

$$[^1(PnP)]_t \simeq K'(e^{-Xt} - e^{-Yt}) = K'(e^{-t/\tau'} - e^{-t/\tau_E'}) \quad (13)$$

P7P also exhibited monoexponential decay kinetics. However, no intramolecular excimer emission was observable at characteristic excimer emission wavelengths. In addition, P7P revealed a temperature dependence of τ' which is markedly different from the other P*n*P compounds in CM (Figure 4): its slight temperature dependence is comparable to that osberved for EP and DP, where no excimer is formed. Therefore, the single exponential ^{1}P decays observed for P7P reflect $k_1' + k_2'$; k_3' does not contribute measurably to the ^{1}P decay. Since P7P does not undergo intramolecular fluorescence quenching, it, too, was considered as a model for $k_1' + k_2'$ in analyses of other P*n*P data. The idea was discarded due to our inability to assess the effect of a ground-state pyrenyl group on the lifetime of a nearby pyrenyl singlet: if the average location and orientation of the pyrenyl groups of P7P place them in proximity (so that the polarization of one is sensed by the other), the fluorescence lifetime may be diminished via acceleration of k_1' or k_2' *without* the occurrence of identifiable quenching. For instance, the lifetime of pyrene in cyclohexane is 450 ns but is reduced to 300 ns in acetone.[49]

Calculation of Rate Constants for Intramolecular P*n*P Excimers in CM and BCCN. As expected for systems described by Scheme I, the intensity of the excimer emission can be described by a noninstantaneous rise and subsequent decay.[46] Depending upon the relative magnitudes of the ^{1}P and ^{1}(P*n*P) lifetimes, the rise

Table II. Lifetime of Alkylpyrenes as a Function of Temperature and Solvent Phase[a]

compd	solvent	lifetimes, ns[b] τ_M (32 °C)[c]	τ_M (70 °C)[c]
EP	CM	160 ± 2 (ch)	147 ± 2 (i)
	BCCN	145 ± 2 (s)	144 ± 2 (n)[d]
	cyclohexane	205 ± 10 (23 °C)	
		237 ± 12 (20 °C)[11]	
DP	CM	147 ± 2 (ch)	136 ± 1 (i)
	BCCN	131 ± 2 (s)	132 ± 2 (n)[d]
	cyclohexane	192 ± 10 (23 °C)	
1-octyl-pyrene[45a]	cyclohexane	225 ± 11	

[a] Cholesteric (ch); nematic (n); smectic (s); isotropic (i). [b] Errors in liquid-crystalline solvents reflect precision. Those in cyclohexane reflect accuracy. [c] Temperatures are ±0.5 °C. [d] Temperature of measurement: ca. 76 °C.

(43) For comparative purposes, we have measured the lifetimes of 10^{-5} M EP and DP in deaerated cyclohexane. Our values are slightly lower than those reported by Thistlethwaite et al.[45a] due to our solvent being spectrograde but not purified further.

(44) (a) Todesco, R.; Gehan, J.; Martens, H.; Put, J.; DeSchryver, F. C. *J. Am. Chem. Soc.* **1981**, *103*, 7304. (b) Van der Auweraer, M.; Gilbert, A.; DeSchryver, F. C. *Nouv. J. Chim.* **1980**, *4*, 153. (c) Meeus, F.; Van der Auweraer, M.; DeSchryver, F. C. *Chem. Phys. Lett.* **1980**, *74*, 218. (d) Halpern, A. M.; Legenza, M. W.; Ramachandran, B. R. *J. Am. Chem. Soc.* **1979**, *101*, 5736. (e) Castellan, A.; Devergne, J.-P.; Bouas-Laurent, H. *Chem. Phys. Lett.* **1980**, *76*, 390. (f) Desvergne, J.-P.; Bitit, N.; Castellan, A.; Bouas-Laurent, H. *J. Chem. Soc., Perkin Trans. 2* **1983**, 109. (g) Wang, W.; Crawford, M. C.; Eisenthal, K. B. *J. Am. Chem. Soc.* **1982**, *104*, 5874.

(45) (a) Snare, M. J.; Thistlethwaite, P. J.; Ghiggino, K. P. *J. Am. Chem. Soc.* **1983**, *105*, 3328. (b) Zachariasse, K. A.; Duveneck, G.; Busse, R. *Ibid.* **1984**, *106*, 1045.

(46) Birks, J. B. "Photophysics of Aromatic Molecules"; Wiley-Interscience: New York, 1970; Chapter 7.

(47) Birks, J.; Alwattar, A.; Lumb, M. *Chem. Phys. Lett.* **1971**, *11*, 89.

(48) Zachariasse, K. A.; Kühnle, W.; Weller, A. *Chem. Phys. Lett.* **1978**, *59*, 375. In the nonviscous solvent, methylcyclohexane, at 20 °C, $k_5' = 4k_4'$ and $k_3' > 50k_4'$.

(49) Alwattar, A. H.; Lumb, M. D.; Birks, J. B. In "Organic Molecular Photophysics"; Birks, J. B., Ed.; Wiley: New York, 1975; Vol. 1, Chapter 8.

Table III. Representative Decay Constants for 10^{-4} M P*n*P in CM and BCCN

compd	solvent	T, °C[a]	phase[b]	τ', ns	τ_D, ns[c]	τ_E', ns[c]
P3P	CM[10]	42.9	ch	113	122	48
	CM[10]	63.0	i	80	84	50
	BCCN	42.2	s	134	132	32[d]
	BCCN		n			~50[e]
P7P	CM	29.1	ch	153		
	CM	64	i			
P10P	CM	37.3	ch	134	138	20
	CM	60.0	i	113	116	23
	BCCN	40.0	s	121	120	8[f]
	BCCN	71.0	n	93	95	25[g]
P13P	CM	40.5	ch	135	143	25
	CM	67.2	i	98	100	29
P22P	CM	44.8	ch	137	140	25
	CM	68.8	i	111	111	31
	BCCN[h]	66.0	n	99	103	35

[a] ±0.5 °C. [b] Nematic (n); smectic (s); cholesteric (ch); isotropic (i). [c] ±5% for $\tau_E' > 30$ ns and ±10% for $\tau_E' < 30$ ns. [d] At 50.3 °C, 34 ns. [e] See text. [f] At 44.7 °C, 9 ns. [g] At 66.0 °C, 25 ns. [h] Insufficient excimer emission to count in the smectic phase.

of the excimer emission may yield the rate constant for either the formation or destruction of the intramolecular excimer.[10] In Table III, the long-time decays of the excimer wave forms in both CM and BCCN, τ_D, are within experimental error of the ^{1}P lifetimes at the same temperature in all of the P*n*P: the rates of formation of the complexes, reflected in the decay portion of the wave forms, are correlated directly with loss of ^{1}P. Therefore, the rise times of the excimer emissions contain τ_E', the lifetimes of the excimer emissions. In practice, each τ_E' can be estimated from a decay constant for monomer emission and the exact time position of a wave-form maximum, t_{max}, by using standard mathematical techniques (eq 14).[50] When τ_E' approaches τ', however, this

$$t_{max} = \frac{\ln (\tau_D/\tau_E')}{(1/\tau_E' - 1/\tau_D)} \qquad (14)$$

simple approximation technique fails. Such a case was observed for P3P in nematic BCCN, where 40.1 ns (74.9 °C) $< \tau' <$ 55.7 ns (55.3 °C). We note only that $\tau_E' \simeq \tau'$ for P3P in nematic BCCN.

Careful examination of the data in Table III reveals that viscosity differences between the cholesteric and isotropic phases of CM have little effect on τ_E'. A similar observation has been reported for P3P in phosphatidylcholine bilayers[7a] and for P10P in several isotropic solvents.[45a] In addition, from comparison of the τ_E', it appears that, as noted by Hirayama for diphenylalkanes in isotropic solvents,[51] P3P forms the most stable excimer in anisotropic media, also. Interestingly, the influence of solvent anisotropy is phase dependent: while τ_E'(P10P) $\simeq {}^1/_2\tau_E'$(P3P) in cholesteric CM, τ_E'(P10P) $\simeq {}^1/_4\tau_E'$(P3P) in smectic BCCN. It appears, therefore, that the highly ordered smectic phase exerts a stronger influence on the P*n*P motions (and/or a greater destablizing influence on the excimers) than does the less ordered cholesteric CM phase.

Determination of Activation Parameters in CM and BCCN. Equation 12 expresses τ' as a function of the monolumophoric rate constants, k_1' and k_2', and the rate constant for intramolecular excimer formation, k_3'. The sum of k_1' and k_2' is given by $1/\tau_M$ of a model compound, EP or DP, and which is essentially temperature independent. Since k_3' can be described by an Arrhenius expression, the temperature dependence of τ' appears in only one of the three rate constants of eq 15. Plots of ln k_3', taken as ln

$$1/\tau' \simeq 1/\tau_M + A_3' e^{-E_3'/RT} \qquad (15)$$

$(1/\tau' - 1/\tau_M)$, vs. $1/T$ yield the energies of activation, E_3', and preexponential factors, A_3', for excimer formation. Such plots for 10^{-4} M P*n*P ($n > 3$) in CM and BCCN, using values of τ_M from 10^{-4} M DP, are shown in Figures 6 and 7. For P3P, τ_M of EP has been used.

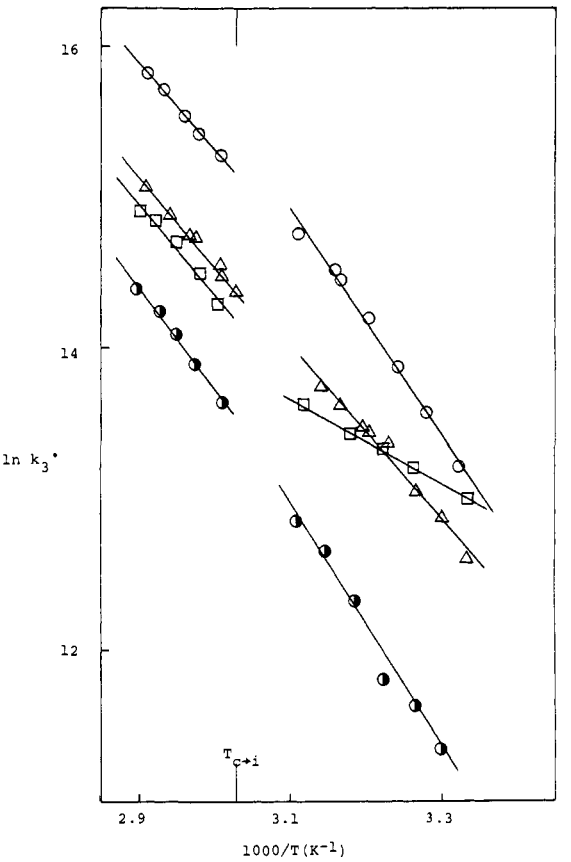

Figure 6. Arrhenius plots of intramolecular fluorescence quenching of 10^{-4} M P*n*P in CM. (○) P3P, (□) P10P, (△) P13P, (◑) P22P.

In CM, the Arrhenius plots constructed in the above manner are reasonably linear within a phase and the points of intersection occur <5 °C from optically detected transition temperatures. However, in BCCN, plots are linear only in the nematic phase. In smectic BCCN, the P3P and P22P plots show marked curvature. The similarity of τ_M and τ' in the low-temperature region introduces large uncertainties in k_3' and may, in fact, be responsible for the curvature in the plots. Alternatively, it is possible that the observed nonlinear Arrhenius behavior may be due to the intervention of an additional, low-temperature mesophase (although this hypothesis is not supported by differential scanning calorimetry[26]) or solvent-related factors which have not been considered.

Values of ΔS^* (calculated from standard Eyring plots), E_3', and A_3' from data obtained in the liquid-crystalline and isotropic phases of CM and BCCN are given in Tables IV and V, respectively.

(50) Birks, J. B.; Dyson, D. J.; Munro, I. H. *Proc. R. Soc. London, Ser. A* **1963**, *275*, 575.
(51) Hirayama, F. *J. Chem. Phys.* **1965**, *42*, 3163.

Talbe IV. Activation Parameters for Intramolecular Quenching of ^1P by P in the Cholesteric and Isotropic Phases of CM

	cholesteric CM[a]				
	P3P[b]	P7P	P10P	P13P	P22P
E_3', kcal mol^{-1}	10.5 ± 0.4	*c*	5.7 ± 0.2	11.5 ± 0.5	16.1 ± 0.4
A_3', s^{-1}	(3.8 ± 2.6) × 10^{13}	*c*	(5.6 ± 1.3) × 10^9	(6.8 ± 5.3) × 10^{13}	(3.1 ± 1.6) × 10^{16}
$\Delta S^{\ddagger}$, eu	1 ± 1	*c*	−16 ± 1	3 ± 2	15 ± 1
	isotropic CM[a]				
	P3P[b]	P7P	P10P	P13P	P22P
E_3', kcal mol^{-1}	11.4 ± 0.2	*c*	11.7 ± 0.9	11.8 ± 0.8	12.9 ± 0.5
A_3', s^{-1}	(1.2 ± 0.3) × 10^{14}	*c*	(7.5 ± 9.6) × 10^{13}	(9.9 ± 11.3) × 10^{13}	(2.3 ± 1.8) × 10^{14}
$\Delta S^{\ddagger}$, eu	4 ± 1	*c*	3 ± 2	4 ± 2	6 ± 2

[a] Activation parameters are calculated by using DP as model compound except where indicated otherwise. Errors are expressed as standard deviations. [b] EP as model.[10] [c] No quenching observed.

Table V. Activation Parameters for Intramolecular Quenching of ^1P by P in Smectic and Nematic BCCN[a]

	P3P[b]	P10P	P22P[b]
		Smectic Phase	
E_3', kcal mol^{-1}		8.1 ± 0.8	
A_3', s^{-1}		(2.2 ± 2.9) × 10^{11}	
$\Delta S^{\ddagger}$, eu		−9 ± 3	
		Nematic Phase	
E_3', kcal mol^{-1}	5.9 ± 0.3	7.1 ± 0.3	9.8 ± 0.5
A_3', s^{-1}	(9.1 ± 3.7) × 10^{10}	(9.2 ± 3.9) × 10^{10}	(4.6 ± 3.4) × 10^{12}
$\Delta S^{\ddagger}$, eu	−11 ± 1	−11 ± 1	−3 ± 2

[a] Values for P10P and P22P activation parameters are calculated by using DP as model compound. For P3P, EP is used. Errors represent one standard deviation. [b] Poor correlations to straight line fits of data in Figure 7 did not warrant calculation of activation parameters. For P3P, r = 0.963, and for P22P, r = 0.947.

Influence of Liquid-Crystalline Media on P*n*P Conformations. Theoretical studies of alkane chain cyclization dynamics[2,52] indicate that in isotropic solvents the most stable ground-state conformers are those in which the vicinal methylenic hydrogens are in a trans orientation. In liquid-crystalline media, fully extended chain conformations are calculated[53a,b] and found[53c-e] to be preferred. Hence, the P*n*P are expected to exist in CM and BCCN mesophases, on average, far from the orientations necessary for intramolecular quenching. Accordingly, formation of the ^1P–P quenching complex requires rotation about at least one C–C bond to change from a more-or-less extended conformation to a more globular, "sandwich"-type complex in which the two pyrenyl moieties are separated by 3–4 Å.[16,42b,54] As concluded by Johnson[55] and others,[33a,c,34,36a,56] molecular dynamics of this type may be strongly influenced by the bulk viscosity and, perhaps even more importantly, by the microstructure of the solvent surrounding the solute (even though solvent molecules can be surprisingly fluid[53b,d,e]). Since the anisotropic nature of the liquid-crystalline mesophases is likely to result in P*n*P solubilization which is quite dissimilar to that in isotropic CM or BCCN, we anticipated phase-dependent activation parameters for quenching.

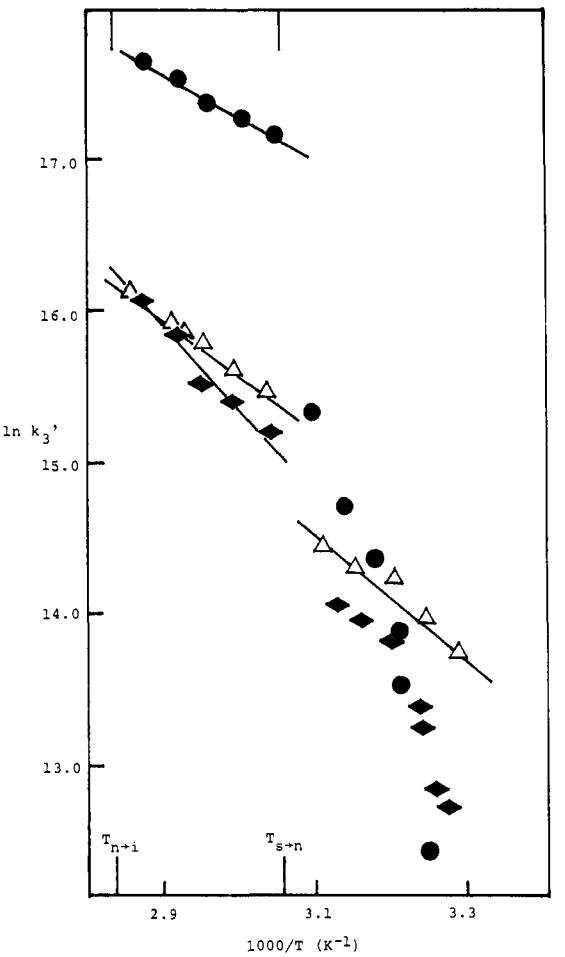

Figure 7. Arrhenius plots of intramolecular fluorescnece quenching of 10^{-4} M P*n*P in BCCN. (●) P3P with EP as model, (△) P10P with DP as model, (♦) P22P with DP as model.

Discussion

Chain Conformations and Flexibility in Mesophases. The pyrenyl singlet lifetimes of P*n*P should approach a constant limiting value as the chain length (and, presumably, the time for one end to find the other) increases. If the singlet lifetime of DP (or EP) represents the long-chain limit of P*n*P, then, as indicated by data in Tables II and III, only in smectic BCCN (in which no excimer emission was detected) and cholesteric CM is there almost no intramolecular quenching for the longest molecule examined, P22P.

The LCICD spectra of P*n*P in CM are consistent with predictions[53] that P*n*P will be extended in the mesophases. From Table I it can be seen that the ellipticity of P10P is larger than those of P3P and P7P but that the absolute ellipticities of the P*n*P (n = 3, 7, 10) are about one-half the values expected upon doubling the ellipticity of DP (i.e., normalizing the concentrations of pyrenyl chromophores). As mentioned previously, these data require that

(52) Flory, P. J. In "Outlook for Science and Technology"; National Research Council, Ed.; W. H. Freeman: San Francisco, 1982; p 370.
(53) (a) Ben-Shaul, A.; Rabin, Y.; Gelbart, W. M. *J. Chem. Phys.* **1983**, *78*, 4303. (b) Oweimreen, G. A.; Martire, D. E. *Ibid.* **1980**, *72*, 2500. (c) Leadbetter, A. J.; Frost, J. C.; Gaughan, J. P.; Gray, G. W.; Mosley, A. J. *Physique* **1979**, *40*, 375. (d) Craven, B. M.; De Titta, G. T. *J. Chem. Soc., Perkin Trans. 2* **1976**, 814. (e) Krishnamurti, D.; Krishnamurthy, K. S.; Shashidhar, R. *Mol. Cryst. Liq. Cryst.* **1969**, *8*, 339.
(54) Birks, J. B.; Lumb, M. D.; Munro, I. H. *Proc. R. Soc. London, Ser. A* **1964**, *280*, 289. (b) Mataga, N.; Torihashi, Y.; Ota, Y. *Chem. Phys. Lett.* **1967**, *1*, 385. (c) Forster, Th.; Seidel, H.-P. *Z. Phys. Chem. (Wiesbaden)* **1965**, *45*, 58. (d) Goldschmidt, C. R.; Ottolenghi, M. *J. Phys. Chem.* **1970**, *74*, 2041.
(55) (a) Johnson, G. E. *J. Chem. Phys.* **1975**, *63*, 4047. (b) *Ibid.* **1974**, *61*, 3002.
(56) (a) Goldenberg, M.; Emert, J.; Morawetz, H. *J. Am. Chem. Soc.* **1978**, *100*, 7171. (b) Okada, T.; Saito, T.; Mataga, N.; Sakata, Y.; Misumi, S. *Bull. Chem. Soc. Jpn.* **1977**, *50*, 331. (c) De Schryver, F.; Demeyer, K.; Huybrechts, J.; Bouas-Laurent, H.; Castellan, A. *J. Photochem.* **1982**, *20*, 341. (d) Halpern, A. M.; Chen, P. P. *J. Am. Chem. Soc.* **1975**, *97*, 2971.

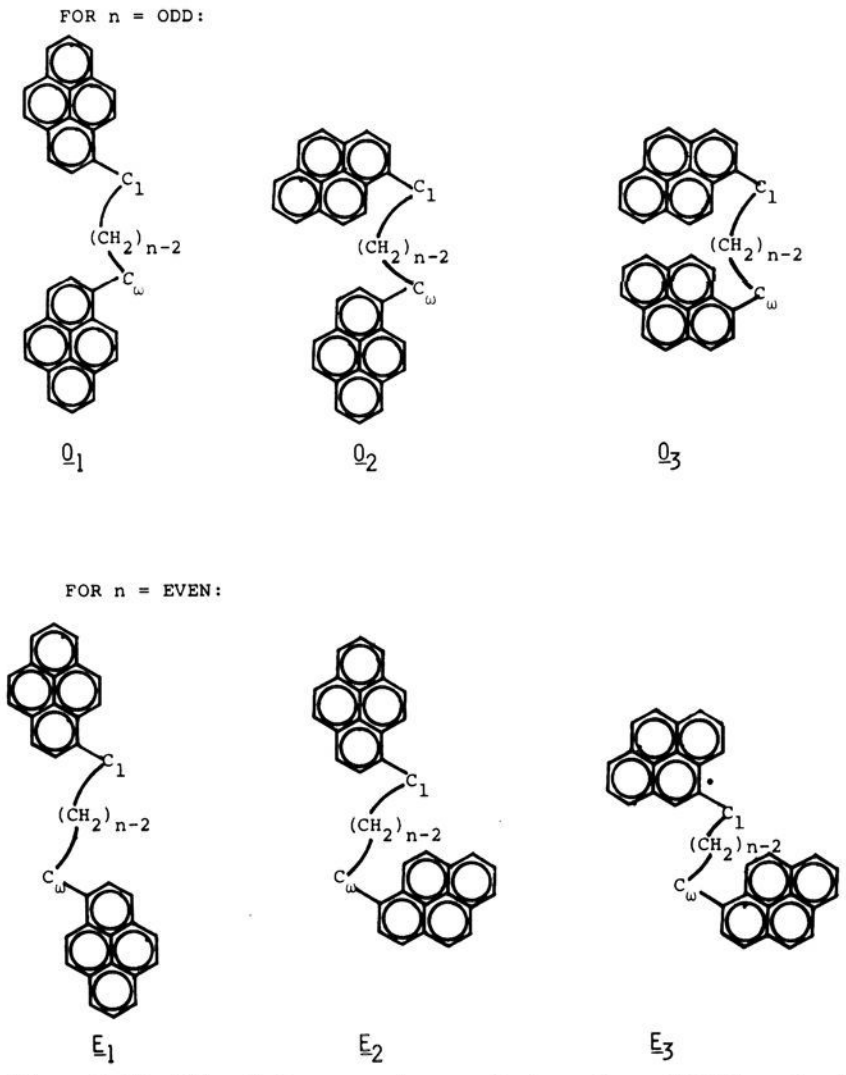

Figure 8. Possible relative pyrenyl–pyrenyl orientations of P*n*P in ordered media.

the alignment of at least one pyrenyl unit with respect to the CM-phase axes be different from that of DP.[57] If the chains are extended, two families of conformers, one for n = even numbers and one for n = odd numbers, exist due to pyrenyl rotations about linkages to the chain. Those extended conformers in which the two pyrenyl groups remain coplanar are shown in Figure 8. A space-filling molecular representation of P3P and P22P in their extended and sandwich conformers is given in Figures 9 and 10. Flanking models of cholesteryl nonanoate and BCCN are included to convey the relative size of each species. As can be seen in Figure 8, some of the rotamers (O_1, E_1, and E_3) place the two pyrenyl groups coparallel (and, therefore, their individual LCICD contributions become completely additive) while others (O_2, O_3, and E_2) do not. If the chains are more-or-less fully extended within the mesophases, then the ellipticity of P10P being slightly larger than that of P3P or P7P can be rationalized qualitatively on the basis that the mole fraction ratio $O_1/(O_2 + O_3)$ for n = odd, is less than $(E_1 + E_3)/E_2$ for n = even. Regardless of the degree of chain extension in the ordered media, we believe that the ellipticity differences can be attributed to differing rotamer populations like those shown in Figure 8.

Application of the Modified Kramers Theory[58] to the Energetics of Intramolecular P*n*P Fluoresence Quenching in CM. Recently, several authors have applied the Kramers theory (which separates intrinsic, solute-localized reaction barriers from extrinsic, solvent-related barriers) to local conformational interconversions occurring in viscous media.[56a,59] Kanaya, Goshiki, Yamamoto, and Nishijima[5] have adapted the theory to apply to intramolecular fluorescence quenching of bis((1-pyrenylmethoxy)carbonyl)alkanes

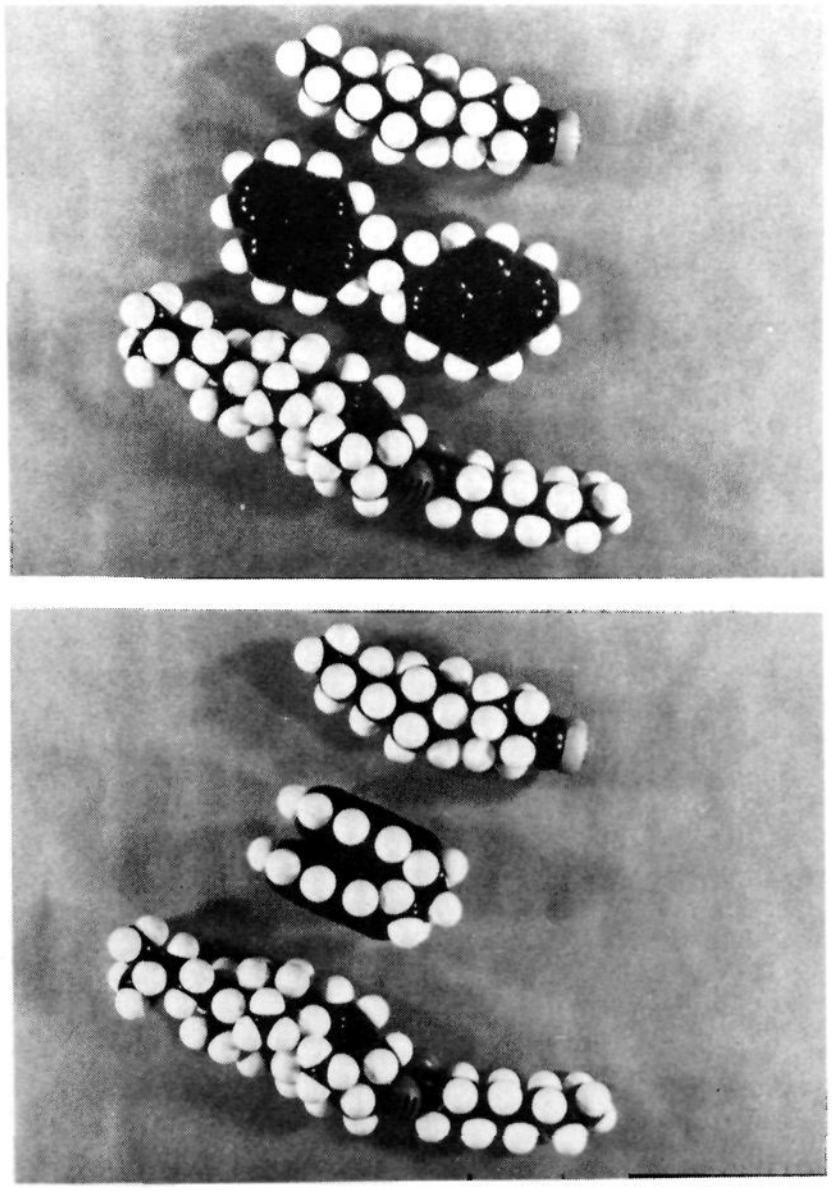

Figure 9. CPK models of extended (a) and sandwich (b) conformers of P3P flanked by BCCN and cholesteryl nonanoate.

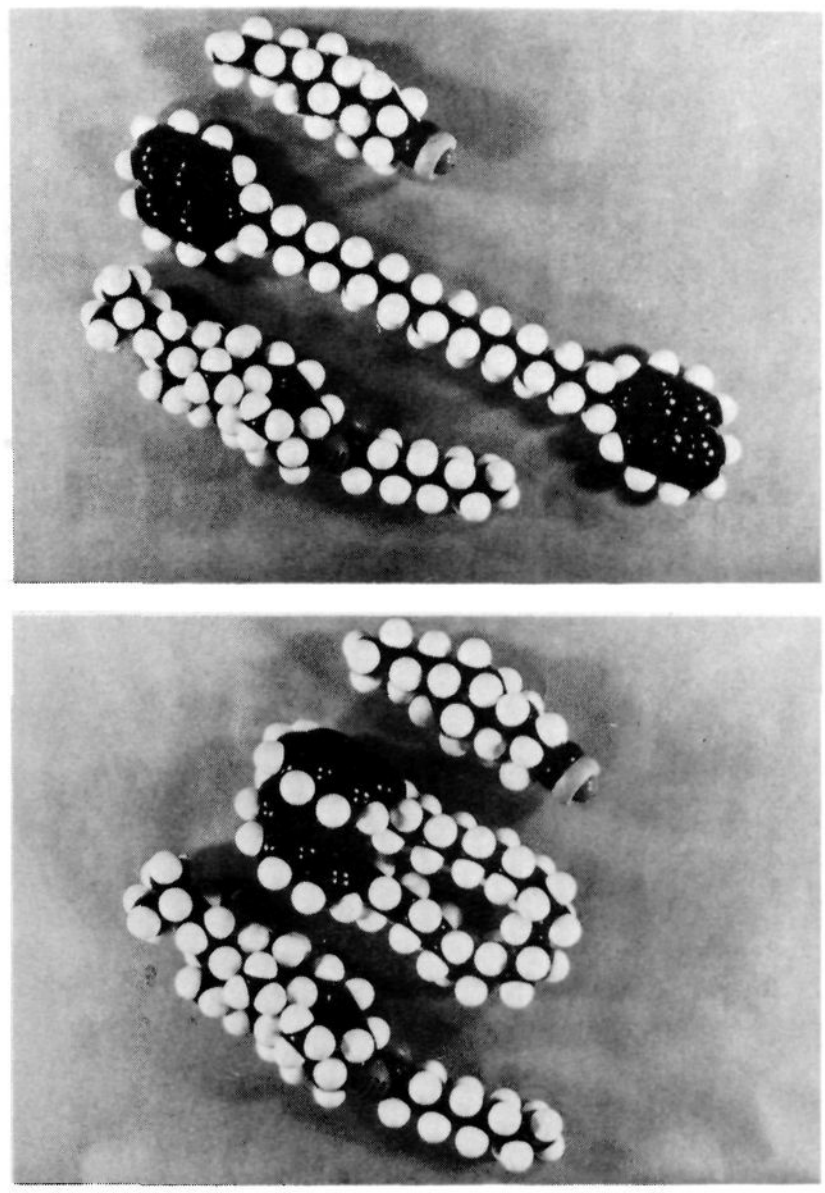

Figure 10. CPK models of extended (a) and sandwich (b) conformers of P22P flanked by BCCN and cholesteryl nonanoate.

(57) Alternatively, the lower P*n*P ellipticities can be ascribed to a greater local disruption of CM solvent order by P*n*P than DP. If this were the case, we expect that the LCICD of P3P would have been much lower than that of P7P. It is not. Further work in this area is ongoing.

(58) Kramers, H. A. *Physica (Amsterdam)* **1940**, *7*, 284.

(59) (a) Lamola, A. A.; Flores, J. *J. Am. Chem. Soc.* **1982**, *104*, 2530. (b) Beece, D.; Eisenstein, L.; Frauenfelder, H.; Good, D.; Marden, M. C.; Reinisch, L.; Reynolds, A. H.; Sorensen, L. B.; Yue, K. T. *Biochemistry* **1980**, *19*, 5147. (c) Beece, D.; Browne, S. F.; Czege, J.; Eisenstein, L.; Frauenfelder, H.; Good, D.; Marden, M. C.; Marque, J.; Ormos, P.; Reinisch, L.; Yue, K. T. *Photochem. Photobiol.* **1981**, *33*, 517.

(BPMC) in a low-viscosity medium, 2-methyltetrahydrofuran (MTF). The activation energies for intramolecular BPMC fluorescence quenching in MTF were found to be independent of the chain length separating the pyrenyl end groups. From this, it was concluded that a single conformational change along the chain is the rate-determining step in the series of motions which bring the pyrenyl groups near one another. Our observation that the activation energies associated with fluorescence quenching of P*n*P (n = 3, 10, 13, 22) in *isotropic* CM (a much more viscous solvent than MTF) are also chain-length independent supports (but does not demand) their hypothesis. However, the lack of quenching in P7P, by itself, may mean that some other P*n*P E_3' values will be chain-length dependent. Considering that factors other than chain rotations may contribute to the P7P observations (e.g., poor pyrenyl–pyrenyl π overlap[48]), the reason for the constancy of E_3' values of the other measured P*n*P and of the BPMC is not totally clear and deserves further attention.

Treatment of our data according to the methodology of Kanaya et al.[5] leads to the conclusion that conformational interconversions of the P*n*P in cholesteric CM are dependent upon factors which are unimportant or nonexistent in isotropic CM: essentially, the Kramers-derived energies parallel those in Table IV. Our results, taken in combination with those from BPMC in MTF,[5] a low-viscosity solvent, confirm that the influence of solvent order upon chain conformational interconversions cannot be ignored: in cholesteric CM, the rate-determining step in intramolecular fluorescence quenching does not appear to be controlled solely by local chain rotation.

The relative ease with which some P*n*P attain a quenching geometry in cholesteric CM as opposed to the difficulty of others requires that the effect of solvent anisotropy on each P*n*P be analyzed separately. There is no apparent correlation between the molecular length of a P*n*P, the average length of the CM constituents (see Figures 9 and 10), and either $\Delta S^{\ddagger}$ or E_3' differences within the cholesteric phase (see Table IV). The solvent fluidity associated with P*n*P bending must be dependent upon a solute's chain length in very subtle ways. One of these may be that on average a P*n*P is nearer the CM component which best approximates its molecular length than existing with equal probability near all three solvent components. Another, as indicated by the low E_3' and large negative $\Delta S^{\ddagger}$ of P10P, is that some chains may be more extended than others or that facile chain motions may be available to some chain lengths in cholesteric CM but not to other. We are attempting to sort these possibilities.[60]

Quenching of P*n*P in BCCN. Plots of ln τ' vs. $1/T$ for P3P, P10P, and P22P vs. $1/T$ in BCCN (Figure 5) are well-behaved. Within a single solvent phase, data points for each P*n*P can be fit relatively well to a straight line. This correlation in smectic BCCN is deceptively simple since manipulating the data to isolate k_3' and plotting it as before (Figure 7) does not result in reasonable fits to straight lines for the P3P and P22P points. Surprisingly, P10P in smectic BCCN exhibits activation parameters which are unexceptional and close to the values calculated from the nematic phase. The curvature of smectic data for P3P and P22P is most likely associated with the large errors introduced in k_3' when τ' of P*n*P is near τ_M of the model alkylpyrene and the two are subtracted. The nearness of τ' and τ_M and the absence of discernible excimer emission demand that there be very little intramolecular quenching of P3P and P22P in smectic BCCN.

The E_3''s in nematic BCCN[61] are not equal and increase regularly with P*n*P chain length (Table V). Given the paucity of data, we cannot determine whether this is a general trend. Regardless, we can state that BCCN mesophase order, like that of CM, affects the ability of P*n*P chains to attain bending conformations in which intramolecular quenching can occur: the activation energies rise as chain length increases instead of decreasing to a constant limit as they do in isotropic solvents.[4,5]

The origin of these effects does not appear to derive from viscosity changes. The similarities between E_3' and $\Delta S^{\ddagger}$ for P10P in nematic and smectic BCCN are more consistent with control by other solvent properties. In effect, the mesophases of BCCN must moderate the efficiency of intramolecular quenching of P*n*P singlets by altering chain bending motions which lead to specific shapes (some of which lead also to quenching).

The smectic B phase of BCCN is highly ordered and expected to be less able than its nematic phase to accommodate a wide variety of chain conformers. Even so, it is possible that large conformational changes of solutes can be promoted at interlayer sites of the smectic phase.[12c] Further discussion of these possibilities and more detailed analysis of the BCCN results must await further experiments.[60]

Conclusion. We have demonstrated that the rates and efficiencies of intramolecular fluorescence quenching in α,ω-bis(1-pyrenyl)alkanes are sensitive to anisotropic environments imposed by liquid–crystalline solvents. Insofar as we have been able to determine, the isotropic phases of the same solvents do not influence the quenching process in an abnormal fashion: that is, the rates and efficiencies of quenching are viscosity and polarity dependent to a similar extent for all chain lengths for which measurements were made. Anisotropic solvent order manifests itself uniquely upon the chain bending of each chain length.

Acknowledgment. We thank Dr. Bruce Craig of the Naval Research Laboratory for his invaluable comments and assistance. Drs. Samir Ghodbane and David Yang of Georgetown University and the referees offered several helpful suggestions and insights. Dr. Klaas Zachariasse graciously supplied samples of P13P and P22P. Dr. Werner Becker of E. Merck in Darmstadt, Germany, donated generous quantities of BCCN. Kay Bayne is thanked for her excellent technical assistance during the manuscript preparation. We are grateful to the National Science Foundation (Grants CHE 7906572 and CHE 8301776) for support of this research.

Registry No. P*n*P (n = 3), 61549-24-4; P*n*P (n = 7), 61549-28-8; P*n*P (n = 10), 61549-31-3; P*n*P (n = 13), 61549-34-6; P*n*P (n = 22), 61549-38-0.

Supplementary Material Available: Two tables of fluorescence lifetimes of P*n*P, DP, and EP in CM or BCCN which encompass the temperatures of the experiments described in this work (3 pages). Ordering information is given on any current masthead page.

(60) Khetrapal. C. L.; Treanor, R. L., II; Weiss, R. G., work in progress.

(61) Force fitting of the smectic phase data leads to E_3'(P3P) $\simeq$ 33 kcal/mol and E_3'(P22P) $\simeq$ 18 kcal/mol but with low correlation coefficients (see Table V).